frontiers | Frontiers in Sustainable Food Systems

TYPE Original Research
PUBLISHED 13 November 2024
DOI 10.3389/fsufs.2024.1464536

OPEN ACCESS

EDITED BY
Poonam Sharma,
Integral University, India

REVIEWED BY
Ovais Qadri,
Thapar Institute of Engineering and Technology, India
Kaiser Younis,
Integral University, India

*CORRESPONDENCE
Ling Dang
✉ dangling1000@163.com
Liangliang Zhang
✉ 703581@sxnu.edu.cn
Yajun Zheng
✉ zyj_coconut@163.com

†These authors have contributed equally to this work

RECEIVED 14 July 2024
ACCEPTED 21 October 2024
PUBLISHED 13 November 2024

CITATION
He C, Dang L, Feng C, Li Y, Zhang L, Zheng Y, Wang N, Liu D and Ye Z (2024) Millet bran dietary fibres treated by heating, dual enzymolysis united with acrylic-grafting or hydroxypropylation: effects on the properties of heat-induced egg white protein gel. *Front. Sustain. Food Syst.* 8:1464536. doi: 10.3389/fsufs.2024.1464536

Millet bran dietary fibres treated by heating, dual enzymolysis united with acrylic-grafting or hydroxypropylation: effects on the properties of heat-induced egg white protein gel

Chenlong He[1†], Ling Dang[2*†], Chen Feng[1], Yan Li[1], Liangliang Zhang[1*], Yajun Zheng[1*], Nan Wang[1], Danhong Liu[1] and Zimo Ye[1]

[1]Food Science College of Shanxi Normal University, Taiyuan, China, [2]Shanxi Technology and Business University, Taiyuan, China

Introduction: Millet bran is an abundant dietary fibre resource, but it is rarely used in Foods.

Methods: To enhance the functional properties and applications of foxtail millet bran dietary fibre (MBDF), MBDF modified by heating, cellulase and xylanase hydrolysis combined with acrylic-grafting (MBDF-HDEAG) or hydroxypropylation (MBDF-HDEH) were prepared, and the effects of these modified MBDFs on heat-induced egg white protein gel (H-EWPG) were studies.

Results and discussion: The results showed that heating and enzymolysis united with acrylic-grafting or hydroxypropylation both enhanced the surface area, soluble fibre content, water-retention and expansion abilities of MBDF. The addition of unmodified MBDF, MBDF-HDEAG and MBDF-HDEH increased the β-sheet content of H-EWPG and made its microstructure denser and granular. Compared with MBDF, MBDF-HDEAG and MBDF-HDEH more effectively improved the gel and texture properties of H-EWPG including water-holding ability (from 20.45 to 34.63 g/100 g), pH (from 4.53 to 7.66), hardness (from 63.92 to 104.53 g), chewiness (from 57.97 to 122.84 g), and gumminess (from 63.92 to 118.18), and a reduction in transparency and springiness ($p < 0.05$). MBDF showed the highest reducing effect on the freeze-thaw dehydration of H-EWPG (from 39.02 to 21.62%). Therefore, addition of MBDFs modified by heating, enzymolysis united with acrylic-grafting or hydroxypropylation can improve gel properties of H-EWPG.

KEYWORDS

millet bran dietary fibre, dual enzymatic hydrolysis, composite modifications, heat-induced egg white gel, gel properties

1 Introduction

Dietary fibre (DF) is essential for human health and it can reduce the occurrence of risk factors such as hypertension, diabetes, obesity, gastrointestinal inflammation, and cancer (Gan et al., 2021). The physicochemical characteristics of DF, especially gel properties, are positively correlated with its soluble dietary fibre (SDF) content, and DFs with an SDF content of over 10 g/100 g are considered to be of high quality (Huyst et al., 2022). The source of DF could

be found in cereal byproducts which are inexpensive and available, but cereal byproduct DFs contain a low content of SDF (approximately 4 g/100 g) (Torbica et al., 2022). Therefore, many studies focus on modification methods that can convert insoluble dietary fibre (IDF) to SDF. These modification methods contained (i) chemical modification includes acidic and alkaline treatments, carboxymethylation, acetylation, and crosslinking, which can modify the chemical composition, structure, and physicochemical properties of DF via changing functional groups (Benitez et al., 2019; Gan et al., 2021; Kanwar et al., 2023); (ii) biological modification contains enzyme hydrolysis and fermentation, which is capable of degrading molecular chains and making hydrophilic groups exposed such as phenolic acid, carboxyl group, and hydroxyl group (Zhu et al., 2019; Jiang et al., 2020); and (iii) physical modifications includes heating, extrusion cooking, ultrafine grinding, ultrasonic treatment, high-pressure homogenization, and extrusion which can break down polysaccharide chains and improve the SDF content (Dong et al., 2022; Tian et al., 2024). Foxtail millet (*Setaria italica*) bran is the main byproduct of millet processing with a high content of DF (55 g/100 g) and annual output (about 5,000 t in China), but millet bran dietary fibre (MBDF) has low SDF content, relatively poor hydration and gelling properties, and limited application in the food industry (Zhu et al., 2019). It has been demonstrated that the SDF content and hydration properties of MBDF can be enhanced by acrylic-grafting or hydroxypropylation (Zheng et al., 2023). Cellulase and xylanse can cause degradation of MBDF and expose hydrophilic groups, because cellulose and hemicellulose is the major of MBDF (Yang et al., 2024). A combination of these approaches may be more effective in increasing the functional properties of MBDF, but the relevant data are limited.

Protein-based hydrogels, especially egg white protein gel, have attracted much attention because of their unique biocompatibility, biodegradability, and easy modification (Li et al., 2022), but the low mechanical strength limits their applications in food, biomedical field, artificial intelligence, and other fields (Grootaert et al., 2022). Egg white protein gel (EWPG) is widely used in food industry but its cost is relatively high. It can be divided into salt-induced, alkali-induced, enzyme-induced, heat-induced, and acid-induced gels according to the particular pre-treatment methods and induction factors involved, and each of them has specific properties (Zang et al., 2023). Heat-induced egg white gel (H-EWPG) has unique gelation properties, such as high elasticity and chewiness, but its hardness, water-retention ability and freeze-thaw property are relatively lower (Lv et al., 2022). Moreover, its high transparency limits its application in preservation of photosensitive food (Lee et al., 2024). It has been shown that the gel characteristics of H-EWPG could be improved and its cost can be lowered by addition of polysaccharides. Previous studies showed that dextran sulfate increased the transparency and water-retention ability of H-EWPG; the mixed gel of carboxymethyl cellulose and ovalbumin had a higher elasticity modulus (Xiao et al., 2020; Liu et al., 2022). Moreover, H-EWPG can be endowed with the functional activities of DFs (such as its hypolipidemic, hypoglycemic, and antioxidation activities) if DFs are added to H-EWG (Zhao et al., 2023), but there has been little research about the effect of DFs on H-EWPG.

Thus, one object of the current study was to research the influence of two composite modification methods (heating, cellulase and xylanase hydrolysis united with acrylic-grafting or hydroxypropylation) on the structure, SDF content and physicochemical characters of MBDF. Moreover, the effects of the modified MBDFs on the gel properties of H-EWPG were studied. This study provides new ways to improve the functional characteristics of DF and egg white gel based food.

2 Materials and methods

2.1 Materials

Foxtail millet bran (*Setaria italica*) was donated by Beiwang Cereal Farm, Qinxian, China. Egg white protein powder (protein content above 95%) was purchased from Zhongyi Egg Co., Ltd., Anhui, China. Cellulase (from Aspergillus niger, 5.0×10^5 U/g), xylanase (from Trichoderma Vride G, 1.5×10^4 U/g), α-amylase (from *Bacillus licheniformis*, 1.0×10^5 U/g), pepsin (5×10^3 U/g, from porcine stomach mucose), and trypsin (from bovine pancreas, 2.5×10^3 U/mg) were from Yigao Chemical Factory, Tianjin, China. Propylene oxide, thiosalicylic acid, sodium chloride, etc. were analytically pure and were purchased from Daimao Chemical Reagent Factory, Tianjin, China.

2.2 Extraction of MBDF

MBDF was extracted using the procedures of Zheng and Li (2018). First, millet bran was milled with a LC-2TX grinder (Xinglin Mill Instrument Factory, Foshan, China) and then sieved with a ZJ-IB2 sifter (Zijing Sifter Machinery Factory, Yiwu, China) to control the particle size to be smaller than 100 meshes. Secondly, the milled millet bran (5 g/100 mL, suspended in 0.1 mol/L of phosphate buffer) and thermostable α-amylase (100 U/g) were incubated at 90°C, 205 rpm and pH 5.0 using a BHE-002Z shaker (Suzhou Shaker Factory, Suzhou, China) for 150 min. Then, Alcalase (100 U/g raw material) was added and the dispersion was incubated at 50°C, 205 rpm and pH 9.0 for 180 min, followed by amyloglucosidase (1,000 U/g raw material) at 60°C, 205 rpm and pH 2.0 for 150 min. The reaction was terminated through heating at 100°C for 10 min. After cooling and filtration, approximately 100 mL of ethanol solution (95%, v/v) was adopted to continuously wash the residue on the filter paper. MBDF was obtained after the residue was dehydrated at 53°C for 7.5 h in a GFGZ-II blast drying oven (Guangdong LANZ Dry Co., Guangzhou, China). Carboxymethyl cellulose was used as the control to determine the soluble millet bran dietary fibre extraction rate.

2.3 Heating and dual enzymes treatment of MBDF

Citing the method of Zheng et al. (2021), MBDF (40 g) was subjected to heat (121.3°C) and high pressure (103.4 kPa) treatment for 45 min using a DZFZ-6C Autoclave (Shandong Boke Instrument Factory, Jinan, China). After the high pressure and temperature treatment, the MBDF was taken out from the Autoclave and then cooled to room temperature. Afterward the MBDF was dispersed in deionized water (1 g/15 mL), and xylanase (60 U/g) and cellulase (40 U/g) were added, which was shaken at 50°C, 205 rpm and pH 5.0 for 150 min. The reaction was terminated via heating treatment (100°C, 10 min). After cooling and filtration, the residue on the filter paper was dehydrated at 45°C using the GFGZ-II blast drying oven. Six hours later, heating and dual enzymes treated millet bran dietary fibre (MBDF-HDE) was obtained.

2.4 Hydroxypropylation of MBDF-HDE

MBDF-HDE dispersion (8 g/150 mL dH_2O, pH 11) was poured into a triangular flask which was placed in a BSZ-20 L water bath shaker (40°C), Na_2SO_4 (mg/mL) and propylene oxide (3 mL) were added in sequence to begin the hydroxypropylation reaction (Zheng et al., 2021). During the hydroxypropylation, the pH of the reaction solution was monitored every half hour, and NaOH (0.1 mol/L) or HCl (0.1 mol/L) was used to ensure that the pH is 11.0. After 27 h of shaking at 195 r/min, the mixture was filtered, and the GFGZ-II blast drying oven (53°C) was used to dry the residue on the filter paper for 5 h. Heat and dual enzymolysis assisted with hydroxypropylation treated millet bran dietary fibre (MBDF-HDEH) was obtained. The substitution degree of hydroxypropyl group was measured citing the procedures described by Shaikh et al. (2019).

2.5 Acrylic-grafting of MBDF-HDE

MBDF-HDE dispersion (2 g/180 mL dH_2O) and 24 mL of NaOH (6.25 mol/L) were poured into a triangular flask which was placed in the BSZ-20 L water bath shaker (25°C), and then 15 mL of acrylic acid (mg/mL) was added to begin the grafting reaction (Rani et al., 2019). After shaking at 185 r/min for 55 min, 2.25 mL of K_2SO_3 (74 mmol/L) and 1.5 mL of thiosalicylic acid (58.4 mmol/L) were added into the dispersion and continuously reacted at 70°C for 3 h. After filtration with nylon fabric (filter diameter of 100 μm), anhydrous ethanol (approximately 30 mL) was employed to wash the residue on the fabric. Then the residue was placed and heated in the GFGZ-II blast drying oven (53°C). Five hours later, heat, dual enzymatic hydrolysis and acrylic-grafting treated MBDF was obtained. The substitution degree of acrylic group was measured citing the method from Rani et al. (2019).

2.6 Preparation of egg white gels with MBDFs

Fifteen grams of egg white powder was dissolved in 100 mL dH_2O and then kept at 4°C overnight. Twenty milliliters of egg white solution was transferred into a 50 mL beaker, and then an amount (1, 2, 3, 4, or 5 g/100 g) of MBDF, MBDF-HDEH, or MBDF-HDEAG (with particle sizes of 18.11–21.58 μm) was added. The mixture in the beaker was gently stirred in the BHE-002Z shaker at 90°C for 30 min. This process included two stages: stirring at 160 rpm for 3 min, and holding for 27 min at 0 rpm (Liu et al., 2022). Finally, the mixtures were cooled under running tap water and kept at 4°C for 7 h to get heat-induced egg white gel (H-EWPG), and heat-induced egg white gels separately fortified with MBDF (H-EWPG/MBDF), MBDF-HDEH (H-EWPG/MBDF-HDEH), or MBDF-HDEAG (H-EWPG/MBDF-HDEAG).

2.7 Chemical constituents, surface area, and colour determinations

The soluble, insoluble, and total dietary fibre contents of MBDF, MBDF-HDEH, and MBDF-HDEAG were determined using the AOAC.991.43 method (AOAC, 2000). The methods including AOAC.955.04, AOAC.920.39, AOAC.924.05 and AOAC.92.05 were employed to determine the ash, protein, moisture, and fat contents of MBDFs (AOAC, 2000), respectively. The acid insoluble lignin, acid and neural detergent fibre contents of MBDFs were determined to separately quantify the hemicellulose, lignin, and cellulose contents (Chu et al., 2019). The surface area ($m^2\ kg^{-1}$) and particle size (Sauter mean diameter, $D_{3,2}$) were analyzed with a JFNER-LB particle size analyzer (Jingbei Frontier Instrument Co., Chengdu, China). Additionally, the colour indexes L (indicative of lightness), b (representative of redness), and a (corresponding to yellowness) of the MBDFs and H-EWPGs were measured with a NH130 High Quality Portable Colour Difference Meter (Three-NH Colorimeter Co., Shenzhen, China). Then, the colour differences (ΔE) between MBDF (/H-EWPG) and the modified MBDFs (/H-EWPGs fortified with MBDFs) were calculated using Equation 1:

$$\Delta E = \sqrt{(L - L_0)^2 + (a - a_0)^2 + (b - b_0)^2} \quad (1)$$

where a_0, L_0, and b_0 are the redness, lightness and yellowness of the untreated MBDF or H-EWPG, respectively.

2.8 Structural investigations

2.8.1 Scanning electron microscopy

First, MBDFs and H-EWPGs were coated with a 10 nm gold layer. Then, the samples were scanned with a scanning electron microscope (JOLE-JMS-5700E, Tokyo, Japan). The accelerating voltage, scale bar, and magnification were 10 kV, 1 μm, and 5,000, respectively (Zheng et al., 2022).

2.8.2 Fourier-transformed infrared spectroscopy

The MBDFs and H-EWPGs were freeze-dried in a vacuum freeze-dryer (HFD-6, Heyuan Ice Equipment Co., Ltd., Zhengzhou, China) and then were scanned with a Fourier-transformed infrared (FT-IR) spectrometer (8400S, Shimadzu, Japan). PeakFit software v4.12 (Seasolve, Framingham, MA, United States) was employed to investigate the secondary structure of H-EWPGs citing the procedure from Bashash et al. (2022). When calculating the secondary structure of egg white protein, the signal peak of cellulose was subtracted from the signal of the mixture.

2.9 Water-retention and expansion abilities and viscosity

Water expansion ability (WEA) and retention ability (WRA) of the samples were determined following the same procedures described by Zheng and Li (2018). The viscosity of MBDFs was measured citing the procedure of Zhu et al. (2019) using a RAV-I5 viscometer (Shengyebao Niandu Instrument Factory, Guangzhou, China).

2.10 Characterization of gels

2.10.1 Water-retention ability

The centrifugation method was adopted to determine water-retention ability (WRA) of the gel samples (Khemakhem et al., 2019).

Briefly, approximately 2 g (M_0) of H-EWGs was added to a centrifuge tube (50 mL), along with filter paper. After filtration at 4,000 × g at 4°C for 20 min, the gel samples were weighed again (M_1). The WRA (%) was calculated according to the Equation 2:

$$\mathrm{WRA}(\%) = M_1 / M_0 \times 100\% \quad (2)$$

where M_0 and M_1 represent the gel weights before and after centrifugation, respectively.

2.10.2 Freeze-thaw cycle test

The gel samples were loaded in a 15 mL glass centrifuge tube for syneresis measurement (Khemakhem et al., 2019). The freeze-thaw cycle contained two steps: (1) the gels in the tube were frozen at −16°C for 24 h; and then (2) the frozen gels were slowly thawed for 8 h at room temperature (approximately 25°C). The gel went through five of these cycles and then weighed (W_s). After filtration (3,500 × g, 15 min), the weight of the residues was measured and record as W_d. Dehydration rate in freeze-thaw cycle was quantified according to Equation 3:

$$\text{Dehydration rate}(\%) = (W_s - W_d) / W_s \times 100\% \quad (3)$$

2.10.3 Optical transparency of gel

Each gel sample was transferred to a quartz colorimetric dish, and the absorbance was determined using a JH754PC UV–Vis spectrophotometer (Shanghai Jinghua Co., Ltd., China) at 600 nm.

2.10.4 Textural properties of gels

The textural properties of H-EWPGs, including hardness, elasticity, cohesiveness, adhesiveness, chewability, and resilience were tested with the TA Plus Texture Analyzer System (LLOYD Instrument Co., HK) with a P/36 R probe. The data were measured in TPA mode, and the test parameters are as follows: the trigger force, compression rate, and test, pre-test, and post-test speeds were 3 g, 50%, 1, 2, and 1 mm/s, respectively (Hou et al., 2022).

2.11 Statistical analysis

Each determination was repeated more than three times. V.17.0 SPSS software (IBM Co., Chicago, America) was employed to analyze the significant differences across data with Duncan's multiple comparisons at a significance level of $p < 0.05$.

3 Results and discussion

3.1 Chemical constituent analysis of MBDFs

The hydroxypropylation degree of MBDF-HDEH and acrylate substitution degree of MBDF-HDEAG were 4.73 and 2.75%, respectively. As shown in Table 1, IDF was the dominant component of MBDF, in which hemicellulose was the main component (57.00 ± 6.23 g/100 g). Zhu et al. (2019) and Zheng et al. (2022) both obtained a similar result. There is no significant difference in fat, ash and protein contents across MBDFs ($p > 0.05$), but a lower IDF content was observed on MBDF-HDEH and MBDF-HDEAG compared with MBDF ($p < 0.05$), corresponding to their higher SDF contents (4.28 and 3.07 g/100 g). After dual enzymolysis and hydroxypropylation or acrylic-grafting, the degradation of hemicellulose and cellulose, and the grafting of hydroxypropyl or acrylic group all can enhance the polarity of MBDF (Shaikh et al., 2019). High pressure and heating (121.3°C, 103.4 kPa) can split polysaccharide chains of DFs and some hydrophilic groups were released as a consequence (Zhu et al., 2019). Alternatively, MBDF-HDEH showed a high SDF content (4.28 g/100 g) which was 4.5 times that of MBDF (0.95 g/100 g), approximately 1.7 times that of heating and cellulase hydrolyzed MBDF (2.49 g/100 g, Zheng et al., 2022) and hydroxypropylated MBDF (2.02 g/100 g, Zheng et al., 2021), revealing that a combination of heating, dual enzymolysis and hydroxypropylation was more effective to increase hydrophilicity of MBDF than any single treatment. Furthermore, a higher SDF content was observed MBDF-HDEH in comparison to MBDF-HDEAG ($p < 0.05$), mainly resulting from the introduced hydroxypropyl group which was more polar than acrylic group (Zheng et al., 2022). The higher SDF contents mean that the modified MBDFs are more effective in increasing the water-holding capacity and sensory quality of gels (Ullah et al., 2019).

3.2 Particle size and colour analysis of MBDF

DFs with large size can bring unacceptable impact on the sensory quality and taste of egg white gel (Zhao et al., 2023). The specific surface area of MBDF was increased but its particle size ($D_{3,2}$) was decreased after the mixed modifications (Table 2), which probably be accounted for the degradation of fibre chains resulting from heating and dual enzymatic hydrolysis (Zheng et al., 2023). An increase in the surface area of DF may enhance its affinity with water or oil molecules, which is helpful to improving gel quality (Ma et al., 2022).

Colour is an important factor affecting DF's application as well as consumer choice. Compared with MBDF, MBDF-HDEH and MBDF-HDEAG both showed a considerable colour difference (ΔE) with a decreased L (representative of lightness) and b values (indicative of yellowness) ($p < 0.05$), indicating that hydroxypropylation and acrylic-grafting both had a negative impact on the colour of MBDF. After heating, dual enzymolysis combined with hydroxypropylation or acrylate-grafting, the degradation of natural pigments under heating and browning reactions occurred during the chemical modification process (Gil-López et al., 2019).

3.3 Structural analysis of MBDF

3.3.1 Surface microstructure

Figures 1A–C reflect the changes in the microstructure of MBDF after the two mixed modifications. MBDF showed a relatively smooth surface microstructure with a small amount of porosity and debris (Figure 1A). In contrast, a distinct honeycomb microstructure with more porosity or debris was observed in MBDF-HEC MBDF-HEPC and MBDF-HEA (Figures 1B,C). Increase in porosity or debris mainly resulted from the breakdown of glycosidic linkages induced by

TABLE 1 Effect of different composite modification methods on the chemical composition, colour, particle size, and hydration properties of MBDFs.

Chemical composition	Millet bran	MBDF	MBDF-HDEH	MBDF-HDEAG
Moisture (g/100 g)	2.69 ± 0.13c	2.86 ± 0.31c	4.45 ± 0.37c	4.57 ± 0.28c
Fat (g/100 g)	6.11 ± 0.56c	2.47 ± 0.37d	3.12 ± 0.35d	2.30 ± 0.95d
Protein (g/100 g)	3.95 ± 0.04c	2.21 ± 0.08d	2.05 ± 0.33d	2.12 ± 0.15d
Ash (g/100 g)	5.55 ± 0.35c	3.07 ± 0.15e	3.71 ± 0.17d	3.46 ± 0.18d
TDF (g/100 g)	69.50 ± 1.20d	88.95 ± 2.06c	86.67 ± 1.68c	87.55 ± 1.36c
SDF (g/100 g)	1.49 ± 0.32f	1.05 ± 0.11e	4.28 ± 0.24c	3.07 ± 0.15d
IDF (g/100 g)	68.01 ± 1.50f	87.90 ± 2.09c	81.39 ± 1.09e	84.48 ± 1.30d
Hemicellulose (g/100 g)	39.61 ± 3.14e	57.00 ± 6.23c	46.47 ± 1.76d	42.87 ± 2.35d
Cellulose (g/100 g)	13.25 ± 0.69e	19.56 ± 1.44c	13.57 ± 0.42d	15.01 ± 1.14d
Lignin (g/100 g)	9.64 ± 0.29c	11.53 ± 0.38c	8.45 ± 0.27d	7.69 ± 0.37d
L	46.66 ± 0.18e	75.22 ± 1.19c	69.15 ± 3.92d	69.16 ± 0.17d
a	6.11 ± 0.09d	8.34 ± 0.30c	7.30 ± 2.45 cd	6.90 ± 0.65d
b	14.92 ± 0.24d	16.00 ± 0.63c	11.66 ± 0.79e	11.60 ± 0.74e
Δ*E*	6.68 ± 0.47d	Control	9.34 ± 2.23c	7.78 ± 1.05d
$D_{(3,2)}$ (μm)	40.25 ± 3.18c	21.58 ± 2.36d	18.56 ± 0.54e	18.11 ± 0.23e
Surface area (cm^2/cm^3)	1905.4 ± 19.00e	2768.63 ± 7.59c	3231.98 ± 11.57d	3226.70 ± 13.99d
Water-holding capacity (g/g)	ND	1.79 ± 0.02e	2.23 ± 0.06d	3.02 ± 0.08c
Water-swelling ability (mL/g)	ND	0.32 ± 0.10e	0.56 ± 0.03d	0.95 ± 0.11c
Viscosity (cP)	ND	12.33 ± 3.79d	18.67 ± 1.4c	19.02 ± 0.52c

MBDF, foxtail millet bran dietary fibre; MBDF-HDEH, MBDF modified by heating and dual enzymolysis combined with hydroxypropylation; MBDF-HDEAG, MBDF modified by heating and dual enzymolysis combined with acrylic-grafting; TDF, total dietary fibre; SDF, soluble dietary fibre; IDF, insoluble dietary fibre. $D_{(2,3)}$: surface-weighted mean particle diameter of MBDFs. ND, not determined. Different small letters (c–f) in the same row indicate significant difference ($p < 0.05$).

heating, dual enzymatic hydrolysis, and alkali treatment during hydroxypropylation and acrylic-grafting (Kanwar et al., 2023).

3.3.2 Fourier-transform infrared spectra

As presented in Figure 2, the untreated and modified MBDFs all had strong peaks approximately at 3340, 2920, 1,600 and 1,050 cm^{-1}, respectively, conforming to the typical FT-IR spectra of dietary fibres. Moreover, changes in several characteristic peaks revealed that heating and dual enzymolysis combined with acrylic-grafting or hydroxypropylation have affected MBDF's structure, especially the chemical bonds and functional groups. In the spectra of MBDF-HDEH and MBDF-HDEAG, the peak at 3397 cm^{-1} in the spectrum of MBDF, which represents the asymmetric stretching of O–H, transferred to 3,337 and 3,334 cm^{-1} after heat and dual enzymolysis united with acrylic-grafting or hydroxypropylation, respectively, indicating that the synthesis modification have changed the hydrogen bonds in MBDF (Ma et al., 2022). The spectra of MBDF-HDEH and MBDF-HDEAG both had a new absorption peak near 910 cm^{-1} (corresponding to the vibration of β–C–H), resulting from the breakdown of β-glycosidic linkages caused by heating and/or dual enzymes hydrolysis (Jiang et al., 2020). In the spectrum of MBDF-HDEH, the red-shift of tiny absorption peak from 1,637 cm^{-1} (representing the vibration of C–H) to 1,604 cm^{-1}, and a new peak appeared at 1427 cm^{-1} (indicating the bending of methyl group), both confirmed the successful grafting of hydroxypropyl group on MBDF (Jiang et al., 2020). Additionally, the new peaks at 1375 cm^{-1} (representing the stretching of C=C bond) and 1,546 cm^{-1} (indicating the vibration of $–COO^-$) suggested that acrylic groups were grafted onto MBDF (Rani et al., 2019). Changes in these typical chemical bonds certificated that the two composite modifications have affected the structure of MBDF.

3.3.3 Crystal structures

The MBDFs' X-ray diffraction spectra and crystallinity values are presented in Figures 3A,B, respectively. MBDF, MBDF-HDEH and MBDF-HDEA exhibited a strong peak at 2θ of 20° (Figure 3A), indicating that they all have cellulose I crystal forms (Ma et al., 2022). The crystallinity of MBDF, MBDF-HDEH and MBDF-HEDEA was not obviously different ($p > 0.05$) (Figure 3B), showing that heating and dual enzymolysis separately united with acrylate-grafting and hydroxypropylation did not significantly affect MBDF's crystal structure (Kanwar et al., 2023), corresponding to their low substitution degree of hydroxypropyl and acrylic groups (4.73 and 2.75%, respectively).

3.4 Hydration properties of MBDFs

Hydration characteristics of DF, including water-retention and expansion abilities, and viscosity, are positively related with their gel properties (Xiao et al., 2020; Ma et al., 2022). Both MBDF-HDEH and MBDF-HEDEA had higher WRA and WEA than MBDF (Table 2). The improvements in WRA and WEA of MBDF after heating and dual enzymolysis separately combined with hydroxypropylation and acrylate-grafting were mainly attributed to two reasons: (i) the more porous and fragmented microstructure (Figures 1B,C) and larger

TABLE 2 Effects of different addition amounts of MBDFs on the colour of heat-induced egg white protein gel (H-EWPG).

Gels	Amount (g/100 g)	*L*	*a*	*b*	Δ*E*
H-EWPG		95.50 ± 0.71d	−2.45 ± 0.28l	4.65 ± 0.69e	Control
H-EWPG/MBDF	1	86.10 ± 2.15e	0.36 ± 0.88hi	6.21 ± 0.20d	10.04 ± 1.08gh
	2	84.95 ± 0.31ef	0.80 ± 0.07g	6.20 ± 0.38d	11.16 ± 0.24fg
	3	83.78 ± 0.62ef	0.95 ± 0.20ef	5.63 ± 0.36d	12.25 ± 0.60f
	4	81.15 ± 0.96f	1.26 ± 0.04de	5.42 ± 0.73de	14.86 ± 0.87ef
	5	82.18 ± 1.32f	0.55 ± 0.06h	3.68 ± 0.92f	13.73 ± 0.17f
H-EWPG/MBDF-HDEH	1	86.62 ± 0.60e	−0.21 ± 0.01k	5.14 ± 0.97de	10.47 ± 0.96gh
	2	82.91 ± 0.83f	1.05 ± 0.20e	6.01 ± 0.55d	13.40 ± 0.20f
	3	81.32 ± 0.44f	1.04 ± 0.04e	5.26 ± 0.37de	14.69 ± 0.33ef
	4	79.81 ± 1.63f	1.11 ± 0.04e	4.09 ± 0.31e	16.10 ± 1.69e
	5	77.30 ± 0.81fg	1.54 ± 0.37d	3.77 ± 1.26f	18.68 ± 0.80d
H-EWPG/MBDF-HDEAG	1	86.43 ± 0.81e	0.20 ± 0.04ij	4.70 ± 1.01e	9.50 ± 0.08h
	2	81.92 ± 0.70f	0.29 ± 0.03ij	2.97 ± 0.06fg	13.95 ± 0.70f
	3	81.87 ± 0.41f	0.30 ± 0.01k	4.02 ± 0.33ef	14.11 ± 0.38ef
	4	79.74 ± 0.96f	0.75 ± 0.02g	2.16 ± 0.22g	16.28 ± 0.95e
	5	79.96 ± 2.70f	1.13 ± 0.13e	1.22 ± 0.11h	16.13 ± 0.60e

Different small letters (d–l) in the same column indicate significant difference ($p < 0.05$).

surface area (Table 2) increased the touching chance between waters and MBDF; and (ii) the grafting of acrylate or hydroxypropyl group enhanced its polarity, resulting in higher WRA and WEA (Zheng et al., 2021; Manzoor et al., 2022). Although with a higher SDF content, MBDF-HDEH exhibited lower ($p < 0.05$) WRA and WEA than MBDF-HEDAG, probably because of the introduction of acrylate group which enhanced the steric hindrance between polysaccharide chains and thus made the structure of cellulose molecules more relaxed in aqueous solution (Rani et al., 2019).

Viscosity is a main index for polysaccharides to form a gel (Zhang et al., 2023). The viscosities of MBDF-HDEH and MBDF-HDAG were higher than that of MBDF (Table 2), in accordance with their larger surface area, higher WRA, SDF content, and WEA, as well their more porous or multichip microstructure (Tables 1, 2 and Figures 1B,C). An improvement in the SDF content means that more fibres can contribute to the viscosity of the aqueous solution; while increases in WRA, WEA, and surface area indicate that the interactions of fibres with water molecules are stronger, enhancing the viscosity of DF (Xu et al., 2023). Moreover, the viscosity of MBDF-HDEH and MBDF-HDEAG were lower than that of the hydroxypropylated MBDF (24.67 cP, Zheng et al., 2021) and MBDF treated by dual enzymatic hydrolysis assisted with acrylate-grafting (18.73 cP, Zheng et al., 2022), respectively, highlighting that a combination of physical, biological and chemical modifications is not the best way to increase viscosity of MBDF.

3.5 Structural characteristics of H-EWPG with MBDFs

3.5.1 Surface microstructure

The scanning electron micrographs of H-EWPG, and H-EWPGs fortified with MBDF (H-EWPG/MBDF), MBDF-HDEAG (H-EWPG/MBDF-HDEAG), and MBDF-HDH (H-EWPG/MBDF-HDEH) at addition amount of 5 g/100 g are shown in Figures 4A–D, respectively. H-EWPG had a smooth surface and relatively rough inner microstructure with many pores (Figure 4A); whereas H-EWPG/MBDF, H-EWPG/MBDF-HDEH and H-EWPG/MBDF-HDEAG all showed a denser and more granular microstructure with a large amount of tiny pores (Figures 4B–D). During the preparation of heat-induced gels, the addition of fibres can provide a skeleton on which the egg white protein can aggregate, which is helpful to the formation of a dense three-dimensional microstructure with tiny pores (Zhao et al., 2023). Moreover, the skeleton structure of fiber matrix can enhance the interactions between egg white proteins and promote them adsorbing on the surface of gels, leading to a granular surface microstructure (Ullah et al., 2019). In comparison with microstructure of H-EWPG/MBDF (Figure 4B), the microstructures of H-EWPG/MBDF-HDEH and H-EWPG/MBDF-HDEAG were all denser with smaller tiny holes (Figures 4C,D), mainly due to their higher water-expansion volume and viscosity (Table 2), which can improve the aggregation of egg white proteins and lead to the formation of a denser gel (Khemakhem et al., 2019).

The microstructures of H-EWPG fortified with MBDF-HDEH at addition amount of 5, 3 and 1 g/100 g are shown in Figures 4D–F, respectively. It is obvious that the microstructure of H-EWPG became more granular and denser, and the holes became smaller as the addition amount increased. This result demonstrated that an increase in dose of fibres can enhance the intramolecular and intermolecular actions across egg white proteins and promote the formation of a denser gel (Xu et al., 2023).

3.5.2 Secondary structure of gels

Figure 5 depicts the α-helix, β-sheet, β-turn, and random coil contents of H-EWPG and H-EWPGs fortified with MBDFs. The β-turn content of H-EWPG significantly decreased ($p < 0.05$), but its

β-sheet content increased after the addition of MBDF, MBDF-HDEH and MBDF-HDEAG. During the formation of heat-induced gels, the structure of egg white protein is destroyed as the temperature increases; then, the stretched polypeptide chains aggregate and form a three-dimensional spatial structure through hydrogen bonds or hydrophobic forces with decreasing temperature (Lee et al., 2024). The addition of MBDFs with considerable WRA and WEA (Table 2) can enhance the interactions of egg white proteins with water molecules and make the structure of gel denser, leading to a higher content of β-sheet (Xu et al., 2023). Additionally, the hydroxypropyl and acrylate groups of MBDF-HDEH and MBDF-HDEAG can increase the hydrogen bonds between polypeptide chains, facilitating the formation of β-sheet or α-helix (Xiao et al., 2020). Moreover, the β-sheet structure is helpful to the interactions between the egg white proteins (Zang et al., 2023), which was another reason for the denser and more granular microstructure of H-EWPG/MBDF, H-EWPG/MBDF-HDEH and H-EWPG/MBDF-HDEAG (Figures 4B–D).

3.6 Physicochemical properties of H-EWPGs

3.6.1 Colour analysis

Table 3 depicts the effects of different addition amounts of MBDFs on the colour of H-EWPG. Overall, the *L* value (representative of brightness) of H-EWPG reduced as the addition of MBDF, MBDF-HDEH and MBDF-HDEA increased; in contrast, the *a* value (representative of redness) of H-EWPG increased with increasing addition amounts of MBDF, MBDF-HDEH and MBDF-HDEAG ($p < 0.05$). Moreover, the addition of MBDF and MBDF-HDEH (1–3 g/100 g) increased the *b* value (indicative of yellowness) of H-EWPG, but this effect was negatively dose-dependent. These results show that the addition of MBDFs darkened the colour of H-EWPG, which was mainly ascribed to two reasons: (i) the addition of MBDFs (belong to polysaccharides) caused carbonyl ammonia reaction during heating-induced gelation of egg white protein (Zang et al., 2023); and (ii) the colour of these MBDFs was relatively brown (Table 2). Compared with H-EWPG, H-EWPG/MBDF-HDEH exhibited the highest colour difference (ΔE) when the addition amount of MBDF-HDEH was 5 g/100 g; followed by H-EWPG/MBDF-HDEAG as the MBDF-HDEAG addition amount was 4–5 g/100 g. After hydroxypropylation and acrylate-grafting, the introduced hydroxypropyl and acrylic groups both can promote the Maillard reaction between the egg white protein and MBDF (Lv et al., 2022), resulting in a darker colour.

3.6.2 WRA of H-EWPGs

Water-holding ability (WRA) is an important property that can affect the quality of EWPG, and it is influenced by the gaps in the gels' network structure and the attraction forces of hydrophilic polymers (Manzoor et al., 2022). The results in Figure 6A showed that the addition of MBDF, MBDF-HDEH, and MBDF-HDEAG improved the WRA of H-EWPG ($p < 0.05$), and the improvement effects were dose-dependent. One reason for this is that these MBDFs all have considerable SDF content and water-holding capacities (1.79–3.02 g/g, Tables 1, 2), which can enhance the affinity of egg white proteins with water (1.04 g/g, Liu et al., 2022). Another reason is that the addition of these MBDFs increased the β-sheet content of H-EWPG (Figure 5) and the number of tiny holes in the microstructure of H-EWPG (Figures 4B–D), which improved the network structure and facilitates the interaction between H-EWPG and waters (Ma et al., 2021). The increase in pores and fragment on microstructure can enhance the interactions of fibres with water molecules (Khemakhem et al., 2019). Furthermore, MBDF-HDEH and MBDF-HDEAG both exhibited greater ability in improving the WRA of H-EWPG than MBDF at 2–5 g/100 g, mainly attributed to the granular microstructures with a large amount of tiny holes (Figures 4C,D), higher SDF content and WRA (Tables 1, 2). Ullah et al. (2019) found that the network structure of tofu gel has been improved by the addition of okara dietary fiber, too.

3.6.3 Pondus hydrogenii of H-EWPGs

Pondus hydrogenii (pH) is one of the factors affecting the formation of EWG, as well as its network structure, texture properties, application range, and shelf life (Manzoor et al., 2022). As shown in Figure 6B, the pH value of H-EWPG was approximately 4.5, which is near the isoelectric point of ovalbumin (the predominant constituent of egg white proteins, Wang et al., 2018). Meanwhile, the pH value of H-EWPG was significantly increased after the addition of MBDF, MBDF-HDEH, and MBDF-HDEAG at 1–5 g/100 g ($p < 0.05$). The gels

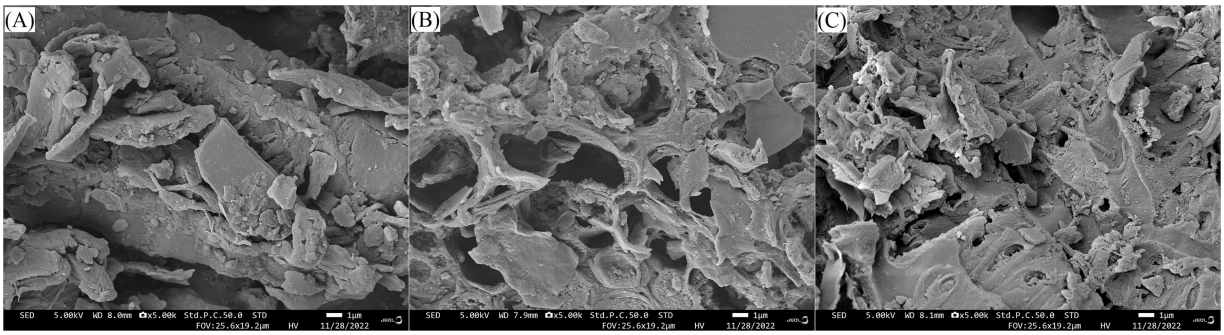

FIGURE 1
Scanning electron micrographs of MBDF (A), MBDF-HDEH (B), and MBDF-HDEAG (C) with a magnification of 5,000×, at 1 μm. MBDF, millet bran dietary fiber; MBDF-HDEH, MBDF modified by heating and dual enzymolysis combined with hydroxypropylation; and MBDF-HDEAG, MBDF modified by heating and dual enzymolysis combined with acrylate-grafting.

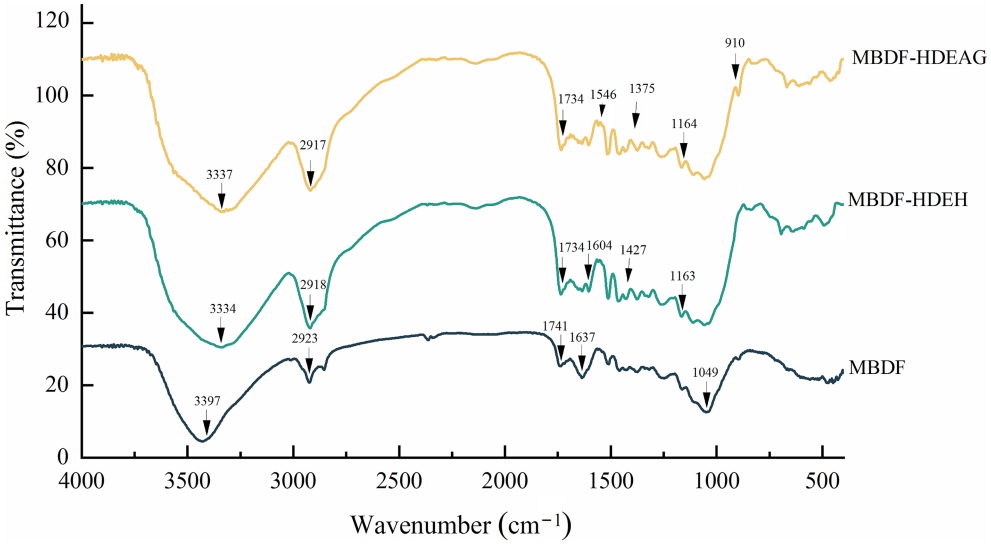

FIGURE 2
Fourier-transformed infrared spectroscopy of MBDF, MBDF-HDEH, and MBDF-HDEAG.

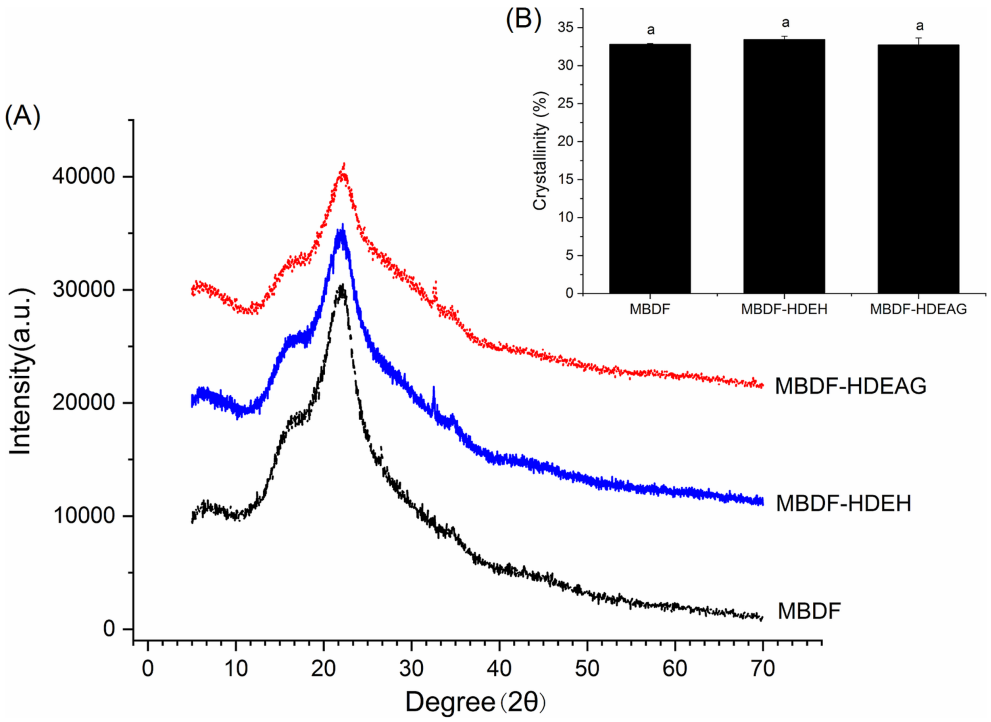

FIGURE 3
X-ray diffraction (A) and crystallinity (B) of MBDF, MBDF-HDEH, and MBDF-HDEAG. Different lowercase letters (a,b) on the bar indicate significant difference ($p < 0.05$).

formed was weak and had low water-holding capacity and transparency at the isoelectric point of egg white proteins, because of the interactions between egg white proteins are low (Zhao et al., 2023); while a dense gel with continuous network structure can be formed between egg white proteins at around pH 7.0 (Khemakhem et al., 2019), which was consistent with the results as shown in Figures 4A–D. Therefore, the addition of MBDFs increased the pH of H-EWPG and thus improved its microstructure. Moreover, the pH values of H-EWPG with MBDF were lower ($p < 0.05$) than that of H-EWPG with MBDF-HDEH or MBDF-HDEAG at 2–5 g/100 g, mainly because of the grafting of hydroxypropyl and acrylic groups, which can change the charge of egg white protein (Shaikh et al., 2019).

3.6.4 Dehydration rate under freeze-thaw cycle

A decrease in dehydration rate of hydrogels under freeze-thaw cycle can help hydrogel-based products to prevent dehydration, hardening, and shrinkage (Bashash et al., 2022). Obviously, the addition of MBDF, MBDF-HDEH, or MBDF-HDEAG (4–5 g/100 g) decreased the dehydration rate of H-EWPG ($p < 0.05$, Figure 6C), indicating their reducing effects in the deterioration of gels during freeze-thaw cycle. The addition of these MBDFs improved the microstructure and water-holding ability of H-EWPG (Figures 4A–D, 6A), and increased the β-sheet content of H-EWPG (Figure 5), leading to a stronger affinity with water molecules under freeze-thaw cycle (Ma et al., 2021). Moreover, the reducing effect of MBDF-HDEH and MBDF-HDEAG on the dehydration rate of H-EWPG was enhanced with increasing addition amount; while the addition of MBDF on the dehydration rate of H-EWPG at 3 g/100 g was higher than that at 4–5 g/100 g. The main reason was that MBDF-HDEH and MBDF-HDEAG had higher SDF content and water-holding abilities (Tables 1, 2), the egg white proteins' aggregation was enhanced and microstructure of H-EWPG became denser with increasing addition amount of MBDF-HDEAG and MBDF-HDEAH (Figures 4D–F), which was not conducive to water lose in freeze-thaw cycle (Lee et al., 2024). By contrast, MBDF had lower SDF content and water-retaining ability (Tables 1, 2). A large addition amount of fibres with lower polarity will reduce the interaction between egg white proteins, and loosen the structure of H-EWPG, thus induce the gel to lose water after freeze-thaw cycle (Ullah et al., 2019).

3.6.5 Optical transparency of H-EWPGs

The results in Figure 6D revealed that the addition of MBDFs decreased the optical transparency of H-EWPG ($p < 0.05$), which was perhaps due to their effects on the structure and pH of H-EWPG. As shown in Figure 6B, the pH of H-EWPG was 4.5 (near the isoelectric point of egg white protein); at this pH value the interactions between egg white proteins were weak and the network structure of gel formed was loose (Figure 4A), thus, the transparency was high (Khemakhem et al., 2019). After the addition of MBDFs, the pH was increased (Figure 6B) and the interactions between egg white proteins and water molecules were enhanced (Figure 6A), which was conducive to the formation of molecularly homogeneous network (Figures 4B–D) and a higher light scattering (Ma et al., 2021), resulting in a lower transparency. Moreover, the hydrophobic force which was a main force to form and maintain heat-induced gels may be reduced by the addition of MBDFs, which was helpful to decreasing the transparency of gels (Han et al., 2022). Additionally, MBDF showed a greater lowering effect on the transparency of H-EWPG than MBDF-HDEH and MBDF-HDEAG; and the improving effect of MBDF was positive dose-dependent, probably due to its lower WHA (Figure 6A) and granular microstructure of H-EWPG/MBDF with a large number of pores (Figures 4B–D). A granular and porous microstructure can increase the scattering of light and thus decrease the gels' transparency (Zhao et al., 2023). A reduction in optical transparency may benefit the applications of H-EWG in protecting photosensitive foods (Lee et al., 2024).

3.6.6 Texture properties of H-EWPG

The addition of MBDF, MBDF-HDEH, and MBDF-HDEAG all enhanced the hardness of H-EWPG ($p < 0.05$) in a dose-dependent manner (Table 3). During the formation of heat-induced gel, MBDFs can provide a carbon skeleton on which the egg white proteins can adsorb and aggregate; then, the crosslink between the proteins and the

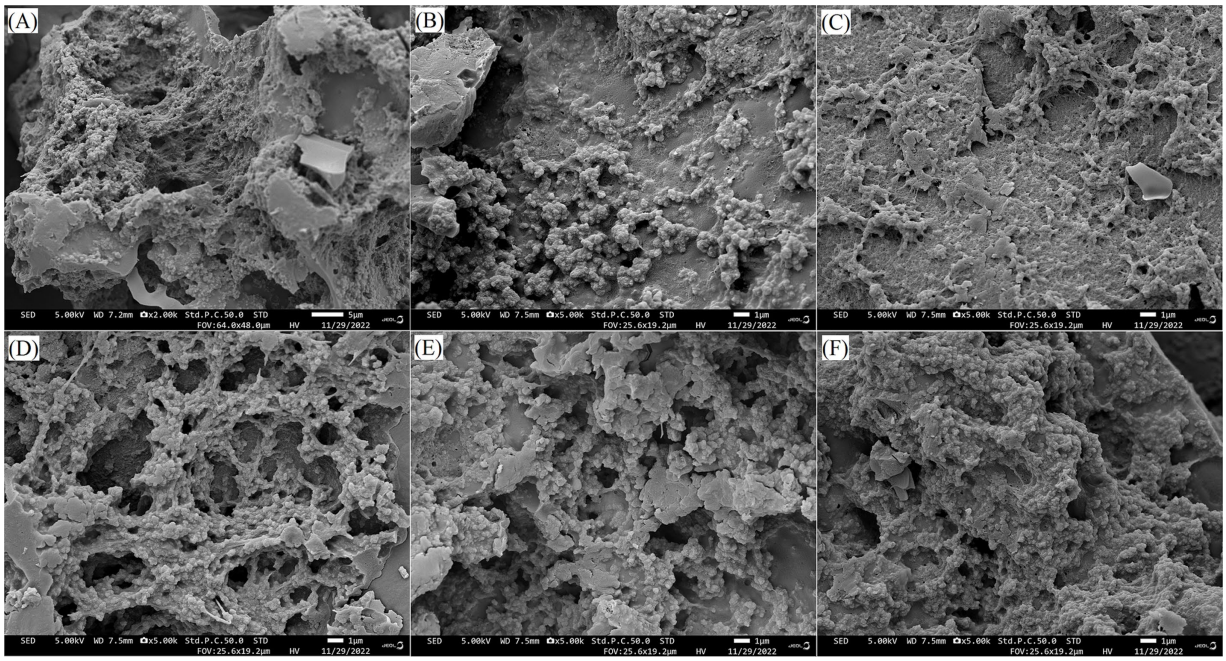

FIGURE 4
Scanning electron micrographs of egg white protein gel (A), egg white protein gel fortified with 5 g/100 g MBDF (B), egg white protein gel containing of 5 g/100 g MBDF-HDEAG (C), egg white protein gel containing of 5 g/100 g MBDF-HDEH (D); egg white protein gel containing of 3 g/100 g MBDF-HDEH (E), and egg white gel containing of 1 g/100 g MBDF-HDEH (F) with a magnification of 5,000×, at 1 μm.

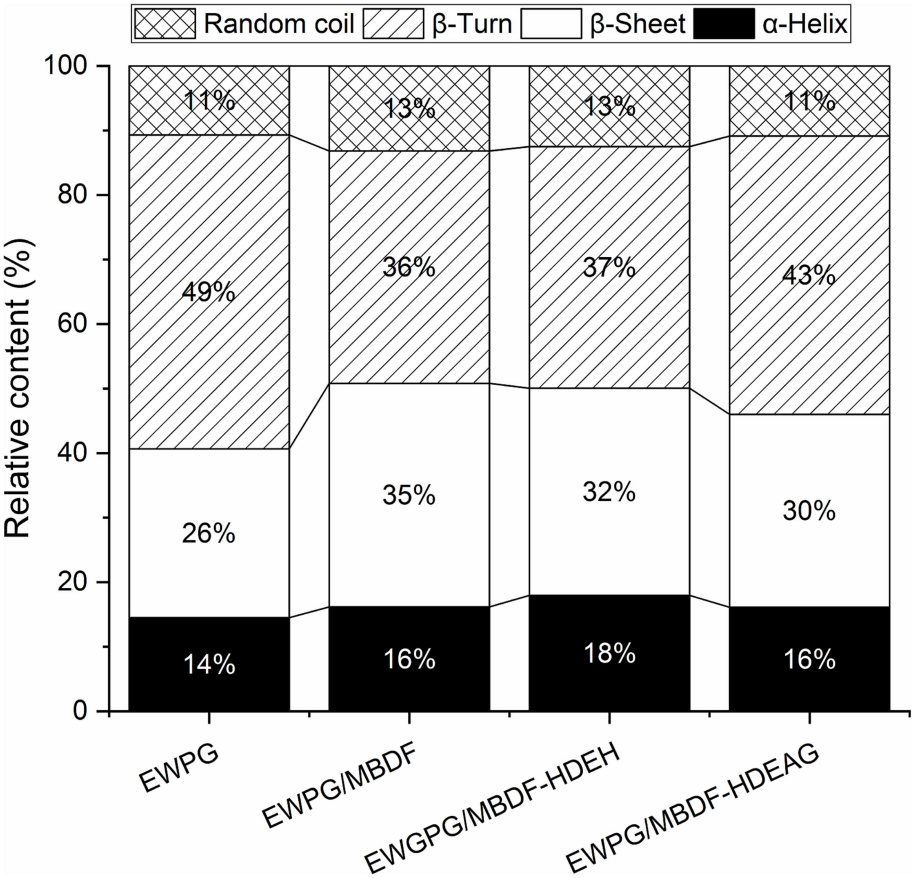

FIGURE 5
Relative content of protein secondary structure of heat-induced egg white gels fortified with MBDFs at addition amount of 5 g/100 g. H-EWPG, heat-induced egg white protein gel; H-EWPG/MBDF; heat-induced egg protein white protein gel with MBDF; H-EWPG/HDEH, heat-induced egg white protein gel containing of MBDF-HDEH; and H-EWPG/HDEAG, heat-induced egg white protein gel with MBDF-HDEAG.

TABLE 3 Effects of different addition amounts of MBDFs on the texture properties of heat-induced egg white protein gel (H-EWPG).

Gels	Addition amount (g/100 g)	Hardness (g)	Springiness	Cohesiveness	Gumminess	Chewiness (g)	Resilience
H-EWPG	0	134.03 ± 3.52g	0.90 ± 0.01a	0.48 ± 0.04a	63.92 ± 3.86d	57.97 ± 2.89e	0.04 ± 0.00a
H-EWPG/MBDF	1	139.93 ± 13.85fg	0.90 ± 0.02a	0.49 ± 0.04a	57.89 ± 5.75d	61.33 ± 0.91e	0.05 ± 0.00a
	2	166.80 ± 15.60e	0.88 ± 0.01a	0.44 ± 0.01b	70.48 ± 6.29cd	64.69 ± 3.66e	0.04 ± 0.00a
	3	216.68 ± 19.16cd	0.88 ± 0.01a	0.44 ± 0.01b	86.20 ± 5.72bc	84.70 ± 4.38c	0.04 ± 0.00a
	4	245.49 ± 17.67bc	0.81 ± 0.03c	0.41 ± 0.03c	86.68 ± 0.06b	82.36 ± 6.71c	0.04 ± 0.00a
	5	258.50 ± 21.90b	0.86 ± 0.01ab	0.43 ± 0.03bc	92.93 ± 5.63b	97.48 ± 6.61bc	0.04 ± 0.00a
H-EWPG/MBDF-HDEH	1	139.53 ± 5.36fg	0.88 ± 0.06a	0.47 ± 0.01ab	68.03 ± 1.75cd	65.54 ± 2.19e	0.05 ± 0.01a
	2	179.09 ± 9.58de	0.88 ± 0.03a	0.44 ± 0.02b	73.33 ± 5.03cd	79.41 ± 9.35d	0.04 ± 0.00a
	3	235.29 ± 9.84c	0.86 ± 0.04ab	0.43 ± 0.02bc	95.28 ± 6.03b	100.24 ± 8.14b	0.04 ± 0.01a
	4	230.15 ± 15.68c	0.86 ± 0.03ab	0.44 ± 0.03bc	101.43 ± 6.12b	100.83 ± 4.32b	0.04 ± 0.00a
	5	260.35 ± 14.17b	0.82 ± 0.06c	0.44 ± 0.01b	118.18 ± 6.47a	112.94 ± 9.65ab	0.04 ± 0.01a
H-EWPG/MBDF-HDEAG	1	203.58 ± 15.22d	0.85 ± 0.05b	0.44 ± 0.02b	76.28 ± 5.52c	89.78 ± 6.06c	0.05 ± 0.01a
	2	235.93 ± 15.85c	0.80 ± 0.04c	0.43 ± 0.03bc	81.42 ± 3.15bc	100.74 ± 11.77ab	0.05 ± 0.01a
	3	232.80 ± 11.03c	0.88 ± 0.06a	0.44 ± 0.02b	88.92 ± 7.99b	101.15 ± 11.34ab	0.05 ± 0.01a
	4	275.51 ± 13.34ab	0.79 ± 0.03c	0.44 ± 0.03bc	94.50 ± 3.98b	119.30 ± 8.71a	0.05 ± 0.01a
	5	288.22 ± 9.54a	0.85 ± 0.01b	0.43 ± 0.02bc	104.53 ± 2.21b	122.84 ± 1.47a	0.05 ± 0.00a

Different small letters (a–f) in the same column indicate significant difference ($p < 0.05$).

gel network strength are both enhanced, resulting in a higher hardness (Zhao et al., 2023). Moreover, the more granular and denser microstructures of H-EWPG/MBDFs with higher water-holding capacity (Figures 4B–E, 6A) enhanced the hardness of gels, too (Ullah et al., 2019). The biggest hardness (288.22 ± 9.54 g) was observed on H-EWPG/MBDF-HDEAG, followed by H-EWPG/MBDF-HDEPH, which was mainly ascribed to their high WRA and denser microstructure (Figures 4C,D, 6A). Additionally, the acrylic group of MBDF-HDEAG and hydroxypropyl group of MBDF-HDEH both can improve the crosslink between hydro polymers (Rani et al., 2019), and thus increase the hardness of H-EWPG.

The gumminess of H-EWPG increased with increasing addition amounts of MBDFs (Table 3). A gel's gumminess represents the energy needed for a semi-solid food to become stable, and it is positively correlated with its hardness, cohesiveness, and viscosity (Zang et al., 2023). It can be speculated that the increased hardness was one reason for the higher gumminess of H-EWPG after the addition of MBDFs. In addition, the higher β-sheet content (Figure 5) also contributed to the high gumminess of H-EWG with MBDFs (Liu et al., 2022). The addition of MBDF-HDEH showed the highest improvement effect on gumminess of H-EWPG, which can be attributed to its high viscosity (Table 2). DFs with high viscosity can improve the hardness and cohesiveness of gels, and enhance the cohesiveness of gels, leading to a higher gumminess (Manzoor et al., 2022).

The chewiness of gels is defined as the product of its gumminess and springiness (Xu et al., 2023); thus, the increased gumminess was mainly responsible for the improvement in the chewiness of H-EWPG after the addition of MBDFs. Additionally, the increase in pH (Figure 6B) and water-holding capacity of H-EWPG (Table 2) were helpful for the formation of a three-dimensional structure with higher chewiness (Li et al., 2023). MBDF-HDEAG showed the greatest enhancing effect on the chewiness of H-EWPG, which was in

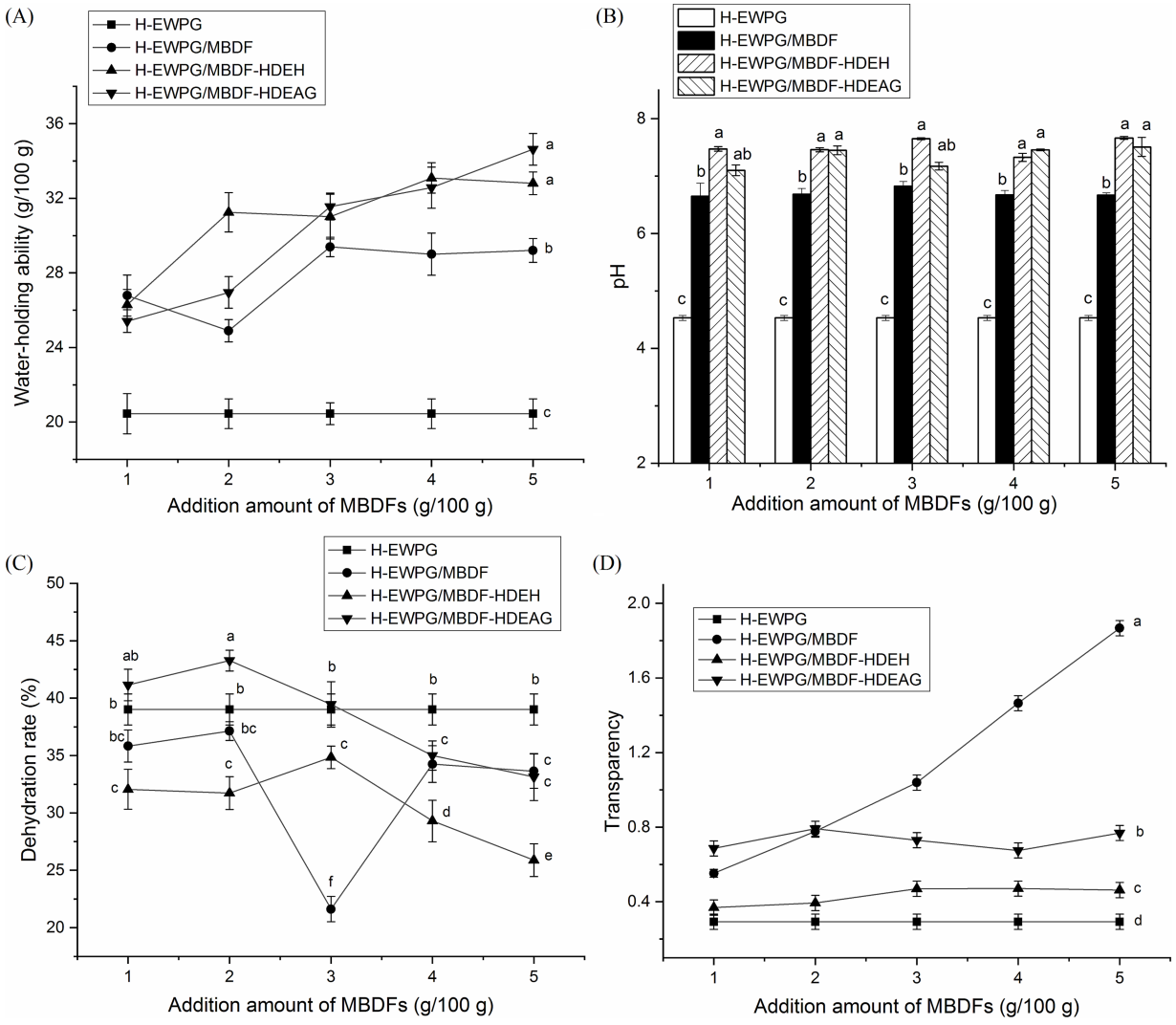

FIGURE 6
Effects of different addition amounts of MBDF, MBDF-HDEH, and MBDF-HDEAG on the water holding ability (A), pH (B), dehydration rate in freeze-thaw cycle (C), and optical transparency (D) of heat-induced egg white protein gel (H-EWPG). Different lower letters (a–e) near the lines or on the bars mean significant difference ($p < 0.05$).

agreement with its highest WRA and WEA (Table 2) and improvement effect on the hardness of H-EWPG (Table 3). An increase in hardness, chewiness, and gumminess means that the applications of H-EWPG in food, biomedicine and cosmetics industries will be expanded (Manzoor et al., 2022).

In contrast, the springiness and cohesiveness of H-EWPG were both reduced ($p < 0.05$) by the addition of MBDF, MBDF-HDEH and MBDF-HDEAG at 2–5 g/100 g. It was found that dietary fibres can increase the strength of gel's network structure via providing a carbon skeleton and/or enhancing the WRA of gels, but reduce their springiness as a consequence (Ma et al., 2022; Zhao et al., 2023). Moreover, the declined β-turn content in H-EWPG after addition of MBDFs (Figure 5) was also responsible for the decrease in springiness of H-EWPG. Protein gels with a high content of β-turn have dense network structure and high springiness (Xu et al., 2023). Cohesiveness is indicative of a gel's tensile strength. After the addition of MBDFs, the hydrophobic forces between protein molecules were reduced (Xiao et al., 2020), and the pH, water-holding capacity, and hardness of H-EWPG were all increased (Figure 6A and Tables 2, 3), which were all disadvantageous to a tight aggregation of proteins (Lv et al., 2022), resulting in a lower cohesiveness. In addition, the addition of these MBDFs did not change the resilience of H-EWPG ($p > 0.05$).

4 Conclusion

Heating, cellulase and xylanase hydrolysis combined with hydroxypropylation or acrylate-grafting enhanced the hydrophilicity, surface area, WRA, viscosity, and WEA of MBDF. The addition of MBDF, MBDF-HDEH and MBDF-HDEAG all made the microstructure of H-EWPG denser and more granular with a large number of tiny pores, and increased its β-sheet content. Moreover, addition of these MBDFs (1–5 g/100 g) increased the WRA and pH of H-EWPG, and reduced its dehydration rate in freeze-thaw cycle, and improved its texture quality, including hardness, chewiness, and gumminess, but lowered its transparency, springiness, and cohesiveness. These results highlight that the addition of MBDFs improved the microstructure and texture quality of H-EWPG, and thus expand its applications in food or other industries. However, these foxtail millet bran dietary fibres' effects on the formation mechanisms and functional properties of H-EWPG need further works.

Data availability statement

The original contributions presented in the study are included in the article/supplementary material, further inquiries can be directed to the corresponding authors.

Author contributions

CH: Investigation, Methodology, Writing – original draft. LD: Methodology, Validation, Writing – review & editing. CF: Data curation, Methodology, Writing – original draft. YL: Funding acquisition, Software, Writing – review & editing. LZ: Validation, Writing – review & editing. YZ: Conceptualization, Funding acquisition, Writing – original draft. NW: Methodology, Software, Writing – review & editing. DL: Validation, Writing – review & editing. ZY: Data curation, Writing – review & editing.

Funding

The author(s) declare that financial support was received for the research, authorship, and/or publication of this article. This research was funded by the Natural Science Foundation of Shanxi Province, China (202203021221139), the Shanxi Graduate Education Innovation Project, China (2023XJG012), and the Innovation and Entrepreneurship Training Program for College Students in 2024, Shanxi Province, China (2024DCXM-55).

Conflict of interest

The authors declare that the research was conducted in the absence of any commercial or financial relationships that could be construed as a potential conflict of interest.

Publisher's note

All claims expressed in this article are solely those of the authors and do not necessarily represent those of their affiliated organizations, or those of the publisher, the editors and the reviewers. Any product that may be evaluated in this article, or claim that may be made by its manufacturer, is not guaranteed or endorsed by the publisher.

References

AOAC (2000). Official methods of analysis. Washington, DC: Association of Official Analytical Chemists.

Bashash, M., Varidi, M., and Varshosaz, J. (2022). Ultrasound-triggered transglutaminase-catalyzed egg white-bovine gelatin composite hydrogel: physicochemical and rheological studies. *Innov. Food Sci. Emerg. Technol.* 76:102936. doi: 10.1016/j.ifset.2022.102936

Benitez, V., Rebollo-Hernanz, M., Hernanz, S., Chantres, S., Aguilera, Y., and Martin-Cabrejas, M. A. (2019). Coffee parchment as a new dietary fiber ingredient: functional and physiological characterization. *Food Res. Int.* 122, 105–113. doi: 10.1016/j.foodres.2019.04.002

Chu, J., Zhao, H., Lu, Z., Lu, F., Bie, X., and Zhang, C. (2019). Improved physicochemical and functional properties of dietary fiber from millet bran fermented by *Bacillus natto*. *Food Chem.* 294, 79–86. doi: 10.1016/j.foodchem.2019.05.035

Dong, R., Liao, W., Xie, J., Chen, Y., Peng, G., Xie, J., et al. (2022). Enrichment of yogurt with carrot soluble dietary fiber prepared by three physical modified treatments: microstructure, rheology and storage stability. *Innov. Food Sci. Emerg. Technol.* 75:102901. doi: 10.1016/j.ifset.2021.102901

Gan, J., Xie, L., Peng, G., Xie, J., Chen, Y., and Yu, Q. (2021). Systematic review on modification methods of dietary fiber. *Food Hydrocoll.* 119:106872. doi: 10.1016/j.foodhyd.2021.106872

Gil-López, D. I. L., Lois-Correa, J. A., Sánchez-Pardo, M. E., Domínguez-Crespo, M. A., Torres-Huerta, A. M., Rodríguez-Salazar, A. E., et al. (2019). Production of dietary fibers from sugarcane bagasse and sugarcane tops using microwave-assisted alkaline treatments. *Ind. Crop. Prod.* 135, 159–169. doi: 10.1016/j.indcrop.2019.04.042

Grootaert, C., Monge-Morera, M., Delcour, J. A., Skirtach, A. G., Rousseau, F., Schymkowitz, J., et al. (2022). Impact of heat and enzymatic treatment on ovalbumin

amyloid-like fibril formation and enzymeinduced gelation. *Food Hydrocoll.* 131:107784. doi: 10.1016/j.foodhyd.2022.107784

Han, T. F., Xue, H., Hu, X. B., Li, R. L., Liu, H. L., Tu, Y. G., et al. (2022). Combined effects of NaOH, NaCl, and heat on the gel characteristics of duck egg white. *LWT* 159:113178. doi: 10.1016/j.lwt.2022.113178

Hou, Y., Liu, H., Zhu, D., Liu, J., Zhang, C., Li, C., et al. (2022). Influence of soybean dietary fiber on the properties of konjac glucomannan/κ-carrageenan corn oil composite gel. *Food Hydrocoll.* 129:107602. doi: 10.1016/j.foodhyd.2022.107602

Huyst, A. M. R., Deleu, L. J., Luyckx, T., Van der Meeren, L., Housmans, J. A. J., Iqbal, S., et al. (2022). Modification of dietary fibers to valorize the by-products of cereal, fruit and vegetable industry—a review on treatment methods. *Plan. Theory* 11:3466. doi: 10.3390/plants11243466

Jiang, Y., Yin, H., Zheng, Y., Wang, D., Liu, Z., Deng, Y., et al. (2020). Structure, physicochemical and bioactive properties of dietary fibers from *Akebia trifoliata* (Thunb.) Koidz. seeds using ultrasonication/shear emulsifying/microwave assisted enzymatic extraction. *Food Res. Int.* 136:109348. doi: 10.1016/j.foodres.2020.109348

Kanwar, P., Yadav, R. B., and Yadav, B. S. (2023). Influence of chemical modification approaches on physicochemical and structural properties of dietary fiber from oat. *J. Cereal Sci.* 111:103688. doi: 10.1016/j.jcs.2023.103688

Khemakhem, M., Attia, H., and Ayadi, M. A. (2019). The effect of pH, sucrose, salt and hydrocolloid gums on the gelling properties and water-retention ability of egg white gel. *Food Hydrocoll.* 87, 11–19. doi: 10.1016/j.foodhyd.2018.07.041

Lee, S., Jeong, S. K. C., Jeon, H., Kim, Y. J., Choi, Y. S., and Jung, S. (2024). Heat-induced gelation of egg white proteins depending on heating temperature: insights into protein structure and digestive behaviors in the elderly *in vitro* digestion model. *Int. J. Biol. Macromol.* 262:130053. doi: 10.1016/j.ijbiomac.2024.130053

Li, Y., Liu, J., Ma, S., Yang, M., Zhang, H., Zhang, T., et al. (2022). Co-assembly of egg white-derived peptides and protein-polysaccharide complexes for curcumin encapsulation: the enhancement of stability, redispersibility, and bioactivity. *Food Chem.* 394:133496. doi: 10.1016/j.foodchem.2022.133496

Li, J., Zhang, W., Tang, T., Gu, L., Su, Y., Yang, Y., et al. (2023). Thermal gelation and digestion properties of hen egg white: study on the effect of neutral and alkaline salts addition. *Food Chem.* 409:135263. doi: 10.1016/j.foodchem.2022.135263

Liu, J. B., Chai, J. J., Yuan, Y. X., Zhang, T., Saini, R. K., Yang, M., et al. (2022). Dextran sulfate facilitates egg white protein to form transparent hydrogel at neutral pH: structural, functional, and degradation properties. *Food Hydrocoll.* 122:107094. doi: 10.1016/j.foodhyd.2021.107094

Lv, Y. Q., Wang, J., Xu, L. L., Tang, T. T., Su, Y. J., Gu, L. P., et al. (2022). Gel properties of okara dietary fiber-fortified soy protein isolate gel with/without NaCl. *J. Sci. Food Agric.* 103, 411–419. doi: 10.1002/jsfa.12155

Ma, Y. Q., Shan, A. S., Wang, R. H., Zhao, Y., and Chi, Y. J. (2021). Characterization of egg white powder gel structure and its relationship with gel properties influenced by pretreatment with dry heat. *Food Hydrocoll.* 110:106149. doi: 10.1016/j.foodhyd.2020.106149

Ma, Z., Yao, J., Wang, Y., Jia, J., Liu, F., and Liu, X. (2022). Polysaccharide-based delivery system for curcumin: fabrication and characterization of carboxymethylated corn fiber gum/chitosan biopolymer particles. *Food Hydrocoll.* 125:107367. doi: 10.1016/j.foodhyd.2021.107367

Manzoor, A., Dar, A. H., Pandey, V. K., Shams, R., Khan, S., Panesar, P. S., et al. (2022). Recent insights into polysaccharide-based hydrogels and their potential applications in food sector: a review. *Int. J. Biol. Macromol.* 213, 987–1006. doi: 10.1016/j.ijbiomac.2022.06.044

Rani, K., Gomathi, T., Vijayalakshmi, K., Saranya, M., and Sudha, P. N. (2019). Banana fiber cellulose nano crystals grafted with butyl acrylate for heavy metal lead (II) removal. *Int. J. Biol. Macromol.* 131, 461–472. doi: 10.1016/j.ijbiomac.2019.03.064

Shaikh, M., Haider, S., Ali, T. M., and Hasnain, A. (2019). Physical, thermal, mechanical and barrier properties of pearl millet starch films as affected by levels of acetylation and hydroxypropylation. *Int. J. Biol. Macromol.* 124, 209–219. doi: 10.1016/j.ijbiomac.2018.11.135

Tian, Y., Sheng, Y., Wu, T., Quan, Z., and Wang, C. (2024). Effects of cavitation jet combined with ultrasound, alkaline hydrogen peroxide and *Bacillus subtilis* treatment on the properties of dietary fiber. *Food Biosci.* 59:103895. doi: 10.1016/j.fbio.2024.103895

Torbica, A., Radosavljević, M., Belović, M., Tamilselvan, T., and Prabhasankar, P. (2022). Biotechnological tools for cereal and pseudocereal dietary fibre modification in the bakery products creation–advantages, disadvantages and challenges. *Trends Food Sci. Technol.* 129, 194–209. doi: 10.1016/j.tifs.2022.09.018

Ullah, I., Hu, Y., You, J., Yin, T., Xiong, S., Din, Z. U., et al. (2019). Influence of okara dietary fiber with varying particle sizes on gelling properties, water state and microstructure of tofu gel. *Food Hydrocoll.* 89, 512–522. doi: 10.1016/j.foodhyd.2018.11.006

Wang, W., Shen, M., Liu, S., Jiang, L., Song, Q., and Xie, J. (2018). Gel properties and interactions of *Mesona blumes* polysaccharide-soy protein isolates mixed gel: the effect of salt addition. *Carbohydr. Polym.* 192, 193–201. doi: 10.1016/j.carbpol.2018.03.064

Xiao, Y., Li, J., Liu, Y., Peng, F., Wang, X., Wang, C., et al. (2020). Gel properties and formation mechanism of soy protein isolate gels improved by wheat bran cellulose. *Food Chem.* 324:126876. doi: 10.1016/j.foodchem.2020.126876

Xu, Y., Qi, J., Yu, M., Zhang, R., Lin, H., Yan, H., et al. (2023). Insight into the mechanism of water-insoluble dietary fiber from star anise (*Illicium verum* Hook. f.) on water-holding capacity of myofibrillar protein gels. *Food Chem.* 423:136348. doi: 10.1016/j.foodchem.2023.136348

Yang, D., Shen, J., Tang, C., Lu, Z., Lu, F., Bie, X., et al. (2024). Prevention of high-fat-diet-induced obesity in mice by soluble dietary fiber from fermented and unfermented millet bran. *Food Res. Int.* 179:113974. doi: 10.1016/j.foodres.2024.113974

Zang, J., Zhang, Y., Pan, X., Peng, D., Tu, Y., Chen, J., et al. (2023). Advances in the formation mechanism, influencing factors and applications of egg white gels: a review. *Trends Food Sci. Technol.* 138, 417–432. doi: 10.1016/j.tifs.2023.06.025

Zhang, T., Yuan, Y. Y., Wu, X. L., Yu, P. X., Ji, J. H., Chai, J. L., et al. (2023). The level of sulfate substitution of polysaccharide regulates thermal-induced egg white protein gel properties: the characterization of gel structure and intermolecular forces. *Food Res. Int.* 173:113349. doi: 10.1016/j.foodres.2023.113349

Zhao, X., Chen, B., Liu, T., Cai, Y., Huang, L., Zhao, M., et al. (2023). The formation, structural and rheological properties of emulsion gels stabilized by egg white protein-insoluble soybean fiber complex. *Food Hydrocoll.* 134:108035. doi: 10.1016/j.foodhyd.2022.108035

Zheng, Y. J., and Li, Y. (2018). Physicochemical and functional properties of coconut (*Cocos nucifera* L) cake dietary fibres: effects of cellulase hydrolysis, acid treatment and particle size distribution. *Food Chem.* 257, 135–142. doi: 10.1016/j.foodchem.2018.03.012

Zheng, Y. J., Li, J. R., Wang, X. Y., Guo, M., Cheng, C. X., and Zhang, Y. (2023). Effects of three biological combined with chemical methods on the microstructure, physicochemical properties and antioxidant activity of millet bran dietary fibre. *Food Chem.* 411:135503. doi: 10.1016/j.foodchem.2023.135503

Zheng, Y. J., Wang, X. Y., Tian, H. L., Li, Y., Shi, P. Q., Guo, W. Y., et al. (2021). Effect of four modification methods on adsorption capacities and *in vitro* hypoglycemic properties of millet bran dietary fibre. *Food Res. Int.* 147:110565. doi: 10.1016/j.foodres.2021.110565

Zheng, Y. J., Xu, B. F., Shi, P. Q., Tian, H. L., Li, Y., Wang, X. Y., et al. (2022). The influences of acetylation, hydroxypropylation, enzymatic hydrolysis and crosslinking on improved adsorption capacities and *in vitro* hypoglycemic properties of millet bran dietary fibre. *Food Chem.* 368:130883. doi: 10.1016/j.foodchem.2021.130883

Zhu, Y., He, C., Fan, H., Lu, Z., Lu, F., and Zhao, H. (2019). Modification of foxtail millet (*Setaria italica*) bran dietary fiber by xylanase-catalyzed hydrolysis improves its cholesterol-binding capacity. *LWT* 101, 463–468. doi: 10.1016/j.lwt.2018.11.052